

Supporting Information for:

Flexible Pores of a Metal-Oxide-Based Capsule Permit Entry of Comparatively Larger Organic Guests

Ayala Ziv,[†] Alina Grego,[†] Sivil Kopilevich,[†] Leila Zeiri,[†] Pere Miro,[‡] Carles Bo,[‡] Achim Müller,[§] and Ira A. Weinstock*,[†]

Contribution from the [†]Department of Chemistry, Ben Gurion University of the Negev, Beer Sheva, 84105, Israel,

[‡]Institute of Chemical Research of Catalonia, Tarragona, Catalonia, 43007, Spain, [§]Faculty of Chemistry, University of Bielefeld, Bielefeld, D-33501, Germany

Contents:

- I. Materials and methods, including the synthesis and characterization of $\text{Na}_{34}[\{\text{Mo}^{\text{VI}}\text{O}_{21}(\text{H}_2\text{O})_6\}_{12}\{\text{Mo}^{\text{V}}\text{O}_4(\text{OAc})_{22}(\text{H}_2\text{O})_{16}\}] \cdot \sim 300\text{H}_2\text{O}$ ($\text{Na}_{34}\mathbf{2} \cdot \sim 300\text{H}_2\text{O}$), and the preparations of solutions for kinetic and other studies.
- II. **Figure S1.** pH-Titration data showing the absence of ammonium acetate in $\text{Na}_{34}\mathbf{2} \cdot \sim 300\text{H}_2\text{O}$.
- III. **Figure S2.** Comparison of the ^{13}C NMR spectra of $(\text{NH}_4)_{42}[\{\text{Mo}^{\text{VI}}\text{O}_{21}(\text{H}_2\text{O})_6\}_{12}\{\text{Mo}^{\text{V}}\text{O}_4(\text{OAc})_{30}\}] \cdot \sim 300\text{H}_2\text{O} \cdot \sim 10\text{CH}_3\text{COONH}_4$, and $\text{Na}_{34}\mathbf{2} \cdot \sim 300\text{H}_2\text{O}$.
- IV. **Figure S3.** Raman spectrum of $\text{Na}_{34}\mathbf{2} \cdot \sim 300\text{H}_2\text{O}$.
- V. **Figure S4.** FTIR and UV-vis spectra of $\text{Na}_{34}\mathbf{2} \cdot \sim 300\text{H}_2\text{O}$.
- VI. **Figure S5.** A representative ^1H NMR spectrum showing how the number of equivalents of acetate in the Na^+ salt of **1** ($\text{Na}_{34}\mathbf{2} \cdot \sim 300\text{H}_2\text{O}$) was determined by quantitative addition of methanesulfonic acid.
- VII. **Figure S6.** A representative ^1H NMR spectrum showing equilibrated exchange between acetate and formate ligands.
- VIII. **Figure S7.** Equilibrium concentrations of acetate and formate inside the complex after incremental additions of formate buffer to $\text{Na}_{34}\mathbf{2}$.
- IX. **Figure S8.** Proton and ^{13}C NMR spectra (in D_2O) of the product obtained by replacement of most of the acetate in $\text{Na}_{34}\mathbf{2}$ by isobutyrate.
- X. **Figure S9.** Proton-NMR spectra of D_2O solutions containing $\text{Na}_{34}\mathbf{2}$ and 45 equiv. of trimethylacetic acid, prepared and maintained both aerobically (in air; 41 days).
- XI. **Figure S10.** Proton-NMR spectra of D_2O solutions containing $\text{Na}_{34}\mathbf{2}$ and 45 equiv. of trimethylacetic acid, prepared and maintained anaerobically (under N_2 ; 25 days).
- XII. **Figure S11.** Progress of reaction (monitored for 60 days by ^1H NMR) for equilibration via ligand exchange of $\text{Na}_{34}\mathbf{2}$ and 33 equiv. of 1,1,1-trimethylacetic acid (1:1 buffer) in air.
- XIII. **Figure S12.** Raman demonstration of the stability of the oxomolybdate complex after undergoing dynamic ligand exchange in solution for 41 days under aerobic conditions (air).
- XIV. **Figure S13.** Numbers of equivalents of acetate and isobutyrate inside and outside the complex during equilibration (from $t = 0$ to 17 minutes after addition of isobutyrate buffer to $\text{Na}_{34}\mathbf{2}$).
- XV. **Figure S14.** Dependence of initial rates of ligand exchange on the concentration of added 1:5 $\text{RCO}_2\text{D}:\text{RCO}_2\text{Na}$ ($\text{R} = \textit{iso}\text{-Pr}$) in D_2O .
- XVI. **Figure S15.** Plot of pH values of an aqueous solution of $\text{Na}_{34}\mathbf{2}$ (50 mg in 0.5 mL water) as a function of added isobutyrate (sodium salt), and brief discussion.
- XVII. **Figure S16.** Effects of adding Na_2SO_4 and NaHSO_4 to D_2O solutions of $\text{Na}_{34}\mathbf{2}$.
- XVIII. Concentrations of $\textit{iso}\text{-PrCO}_2\text{D}$ in solution before and after the first 60 seconds.
- XIX. **Table S1.** Concentrations of species at $t = 0$ (after mixing all components).
- XX. **Table S2.** Concentrations of species after 60 seconds of reaction.
- XXI. **Figure S17.** Plot of $\textit{iso}\text{-PrCO}_2\text{D}$ concentrations before and after 60 seconds.
- XXII. **Figure S18.** Eyring plot and discussion of temperature-dependence data obtained at constant $[\text{Na}_{34}\mathbf{2}]$ and $[\text{RCO}_2\text{D}]$, from 3 rate constants calculated from initial rates at 26, 34 and 56 °C.

I. Materials and Methods

Materials and reagents. Regenerated-cellulose dialysis membranes (45-mm flat-width tubes; 12-14000 Dalton MWCO) were purchased from VWR Scientific, treated before use to remove glycerin and traces of sulfur compounds, and stored under high-purity water (18.2 M Ω , Millipore[®]) at 5 °C. Formic acid (98%; Riedel-de Haën) and isobutyric acid (>99.5%; Fluka) were both distilled before use through a column packed with glass Rasching rings. Trifluoroacetic acid (99%; Acros), trifluoroacetic acid-D (99.5% D; Cambridge Isotope Laboratories, Inc., USA, CIL), acetic acid-D₄ (99.5% D; CIL), deuterium oxide (99.9% D; CIL), ammonium acetate (ACS, Mallinckrodt), ammonium molybdate 4-hydrate (ACS; Mallinckrodt), and hydrazine sulfate (>98%; Fluka) were used as received. All reactions were carried out in 18.2 M Ω water or D₂O.

Instrumentation and spectroscopy. pH Measurements. pH values were measured using a EuTech pH 510 Bench-Top pH meter, or a TES-1380 pH meter equipped with a Ag/AgCl electrode (Thermo Electron, UK), and temperature compensation. Prior to use the pH meter was calibrated using standard reference solutions (pH 4.00 and 7.00). UV-vis spectra were acquired using a Hewlett-Packard 8452A spectrophotometer equipped with a diode-array detector. For all measurements the solutions were diluted as needed to avoid over-saturation by the strongly absorbing ligand-to-metal charge transfer bands of the polyoxometalates in the 190-300 nm region. Proton and ¹³C NMR spectra were acquired on Bruker 200 and 500 MHz spectrometers, and the HDO signal in D₂O samples was used as an internal reference (relative to TMS). Spectral data were processed using the NMR software package, Mnova version 5.1. Fourier-transform infra-red (FTIR) spectra were acquired using a Nicolet Impact 410 spectrophotometer (KBr pellets). The Raman instrument used comprised a Jobin-Yvon LabRam HR 800 micro-Raman system, equipped with a liquid-N₂-cooled detector. The excitation source was a He-Ne laser (633 nm) with a power of 5 mW on the sample. The laser was focused with an x50 long-focal-length objective on the solid sample, to a spot of about 2 μ m. The measurements were taken with the 600 g mm⁻¹ grating and a confocal microscope with a 100- μ m hole. In order to prevent photochemical processes induced by the laser its intensity was reduced by 100 using ND filters.

Synthesis of Na₃₄[Mo^{VI}₇₂Mo^V₆₀O₃₇₂(CH₃CO₂)₂₂(H₂O)₈₈] \cdot ~300H₂O (Na₃₄2). The NH₄⁺ salt of **1** (4.0 g, 0.14 mmoles) was dissolved in ca. 10 mL of 18.2 M Ω water. This solution was transferred to ca. 8 to 10 cm of a 4-cm width regenerated cellulose dialysis membrane (12000 M Dalton cutoff; pre-treated as described above). The membrane was sealed with two clips (the lower one was weighted to keep the membrane immersed), places in a solution of 500 mL of aqueous acetate buffer (1:1 Na⁺: H⁺ forms; 4 M in acetate) and stirred slowly, using a magnetic stir bar, for 13 hours in air (control experiments described below showed that anaerobic conditions were not necessary). The immersed dialysis tube was then placed in 500 mL of pure water and stirred for one hour. This was done a total of 6 times (six hours in total). The solution was then concentrated to dryness by rotary evaporation in warm (40°C) water, to give Na₃₄[Mo^{VI}₇₂Mo^V₆₀O₃₇₂(CH₃CO₂)₂₂(H₂O)₈₈] \cdot ~300H₂O, (Na₃₄2), as a dark red solid. Yield: 3.8 g (95%). ¹H-NMR (D₂O; referenced to HDO at 4.65 ppm relative to external trimethylsilane) δ ppm (intensity; $\Delta\nu$ 1/2 Hz), 0.73 (1, 48), 1.93 (0.03, 4). ¹³C NMR, δ : 23 ppm and 180 ppm., Raman, IR (KBr pellet) and UV-Vis: see Figures S3 and S4, respectively. Anal.: Calcd. (found) for Na₃₄[Mo^{VI}₇₂Mo^V₆₀O₃₇₂(CH₃CO₂)₂₂(H₂O)₈₈] \cdot ~300H₂O: H, 3.07 (2.92), C, 1.91 (1.97), N, 0 (trace), Na, 2.82 (2.60), Mo, 45.75 (42.6). These values were obtained at Galbraith Laboratories, Knoxville, TN, USA. For Mo, a value of 43.6% was found at Ben Gurion University's atomic absorption spectroscopy laboratory.

Comments on the Empirical Formula. The elemental analysis data gave reasonably good fits when the total %-acetate was varied slightly (from 20 to 24 equivalents per complex). Therefore, an independent method (see immediately below) was used to help determine the number of acetate ligands, and by inference, the number of corresponding Na⁺ cations. That data was then used to refine the empirical formula provided here. An additional complication encountered in assigning the molecular formula is that the complex acts as a weak "poly" aqua acid at acetate-buffer pH values. In addition, the total number of waters of hydration (in the isolated, solid product) is large. However, the combined ¹H, ¹³C, Raman, FTIR, and UV-vis data definitively confirmed the structural integrity of the Mo₁₃₂ framework.

The empirical formula of Na₃₄2, Na₃₄[Mo^{VI}₇₂Mo^V₆₀O₃₇₂(CH₃CO₂)₂₂(H₂O)₈₈] \cdot ~300H₂O, may also be written as, Na₃₄[{Mo^{VI}₆O₂₁(H₂O)₆}]₁₂{(Mo^V₂O₄)₃₀(OAc)₂₂(H₂O)₁₆}] \cdot ~300H₂O, in which 16 coordination sites on 16 Mo(V)

centers are occupied by a total of 16 aqua ligands, rather than by 8 acetate ligands. However, these are only a fraction of the total numbers of water present, both coordinated to the 34 Na⁺ counter cations and elsewhere.

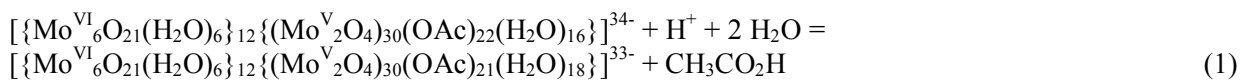
NMR Determination of the Number of Acetate Ligands in the Na⁺ salt 1. Methane sulfonic acid (MSA) 17.3 μ L (0.0257 g, 0.267 mmol) was dissolved in 3.430 g of D₂O (3.07 mL). The final concentration of MSA was 86.5 mM. Then, 500 μ L of this solution (43.25 μ mol) was combined with 50 mg (1.81 μ mol, 3.63mM) of Na⁺ **1** salt. The total number of equivalents of acetate in the system was then calculated from the ratios of ¹H NMR signal intensities. To increase accuracy, the experiment was repeated four times (i.e., four different samples of **1**), using two different MSA solutions. The number of moles of **1** was determined by elemental analysis. (Although the organic component of the Na⁺ salt of **1** is relatively small, such that elemental analysis alone is not sufficiently precise, the molecular weight of the Na⁺ salt is sufficiently large that uncertainty in the number of moles of **1** present in this NMR procedure was small.) The number of equivalents of acetate in each solution was then determined by quantifying the sum of acetate -CH₃ ¹H signal intensities inside and outside **1**, relative to the intensity of the -CH₃ ¹H signal of MSA. The results gave four values for the number of equivalents of acetate associated with each complex: 22.4, 22.6, 22.5 and 21.9 (average = 22.3). A value of 22 acetates per oxomolybdate cluster was used for the empirical formula.

pH Titration of the (NH₄)₄₂1. 1.5056 g (54.6 micromol) of **1** (NH₄⁺ form) was dissolved in 15 mL of 18.2 M Ω water to give a 3.56 mM solution, and the pH was then measured. Methane sulfonic acid (MSA) (100 microL, 0.148 g, in 1 mL of water; 1.40 M) was then added in 85 microL aliquots, and the pH was measured after each addition.

pH Titration of Na₃₄2. The Na⁺ salt (0.3 g, 10.9 micromol) was dissolved in 3 mL of 18.2 M Ω water to give a 3.61 mM solution, and the pH was then measured. A concentrated solution of MSA (100 microL, 0.148 g, in 1 mL of water; 1.40 M) was added in 185 microL aliquots, and the pH was measured after each addition.

Addition of CD₃CO₂D to D₂O Solutions of Na₃₄2. To determine whether the acetate ligands of the Na⁺ salt of the molybdate complex are labile and enter into reversible dissociation equilibria in water, 10 mg (0.156 mmol) of CD₃CO₂D were added to 508 μ L of a D₂O solution containing 50 mg (1.81 μ mol) of Na₃₄2. The ratio of CD₃CO₂D to oxomolybdate was 86, and the total number of equivalents of acetate/complex (CD₃CO₂D + CH₃CO₂⁻) was equal to 108. Using the value of 22 equivalents of CH₃CO₂⁻/complex (quantified by use of an internal NMR standard; see comments above on the empirical formula), and assuming 30 possible acetate coordination sites within the capsule-like complex, the population of ligands inside the complex at equilibrium should be (86/108)30 = 24.8 CD₃CO₂⁻, and (22/108)30 = 6.2 CH₃CO₂⁻. Because only 6.2 of the CH₃CO₂⁻ ligands remain inside the capsule, 22-6.2, or 15.8 equivalents must be expelled. Hence, at equilibrium, the ratio of concentrations of protic acetate outside/inside the capsule is 15.8/6.2 = 2.5.

The experimentally observed value (i.e., in Figure 3) is 3.1. However, the pH (pD) of the solution after adding CD₃CO₂D drops from ca. 5 to 2.9 (pH meter reading). We have observed that decrease in pH(D) shifts the position-of-equilibrium from bound towards dissociated ligands (eq 1). This effect is clearly seen in Figure S5 (below).



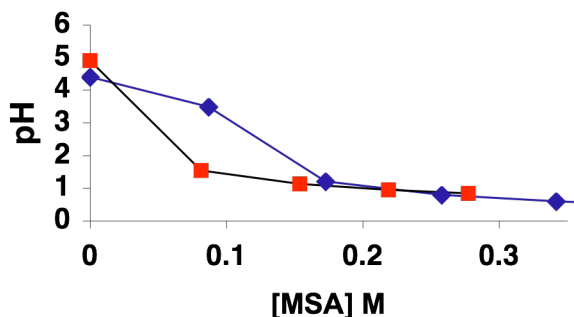
If the above calculation is done assuming that at the lower pH(D), 27 bidentate ligand sites, rather than 30, are now populated inside the capsule, then: (22/108)27 = 5.5 CH₃CO₂⁻ ligands are present at equilibrium inside the capsule, and 22-5.5 = 16.5 are left outside. Hence, the ratio of CH₃CO₂⁻ outside/inside = 16.5/5.5 = 3. We believe this explains the data. Confirmation using buffered solutions of e.g., 1:1 H⁺:Na⁺ forms of CD₃CO₂⁻ was not deemed necessary because the main point, that the acetate ligands in the complex are labile and reversibly dissociate in solution, is clearly demonstrated.

Ligand Exchange by Formate. Purified Formic acid 2.44 g (2.0 mL, 0.053 mol), was mixed with 2.2 mL of 12.06 M NaOH solution (0.0265 mol NaOH). A buffer solution (with 1:1 ratio salt to acid) was obtained. Then 4.5 μ L aliquots of the formate buffer were added to an NMR tube containing 1.8 μ mol of Na₃₄1 in D₂O (50 mg in 0.5 mL D₂O; 3.63 mM). After each addition, an NMR spectrum was acquired. Ratios of signal intensities were converted to numbers of equivalents of acetate or formate, using the total number of equivalents of acetate in the system (22 per equiv. of **2**) as an internal “standard”.

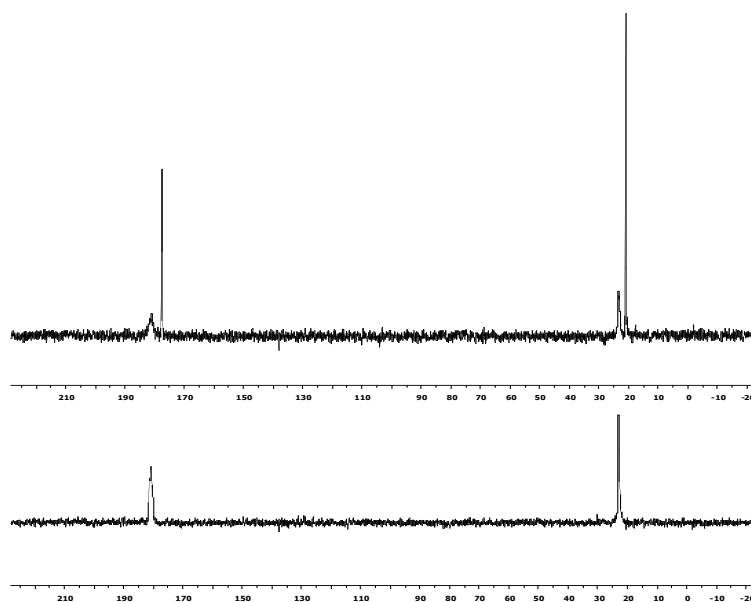
Ligand Exchange by Isobutyrate. Na₃₄2 (50 mg, 1.8 μmol) was combined with 45 equivalents of isobutyrate buffer (1:1 H⁺:Na⁺) in 0.5 mL of D₂O (final concentration of Na₃₄2 was 3.55 mM). After one day, the solution was purified by membrane dialysis against pure water for 90 minutes, and then concentrated to dryness by rotary evaporation. The final solid was dissolved in D₂O and characterized by ¹H and ¹³C NMR. Most, but not all, of the acetate was replaced by isobutyrate (Figure S8).

Stability Studies. Two identical solutions were prepared in parallel, one under air, and the second under N₂ with scrupulous exclusion of dioxygen. These were then evaluated at regular intervals by ¹H-NMR. For both a 1:1 Na⁺:H⁺ buffer solution of 1,1,1-trimethyl acetic acid was made by adding 10 μL of NaOH in D₂O solution (12.06 M, 0.121 mmol) to 0.0245 g (0.240 mmol) of the acid, followed by addition of D₂O until the total volume of the solution was 1.5 mL. To this solution was added 150 mg of Na₃₄2 (5.42 μmol, 3.61 mM), and 0.5 mL of this solution was transferred to a 5 mm NMR tube. For the anaerobic experiment, the final solution was de-aerated by three freeze-pump-thaw cycles, transferred to 5-mm NMR tube under N₂, and in a N₂-filled Schlenk flask under N₂ for the duration of the 41-day experiment. The NMR tube containing the aerobic sample was prepared open to the air, and was stored on the bench under air in a gently capped NMR tube. *After 41 days, the solutions were effectively identical to one another by both ¹H NMR and Raman spectroscopy.*

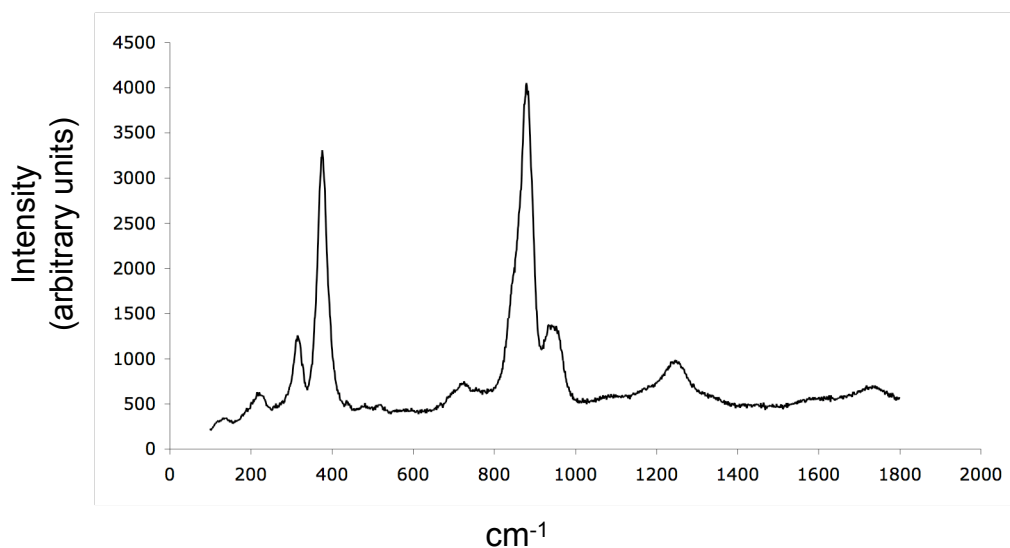
Preparation of the Solutions for the Kinetic Study in Figure 6 (Text). Sodium isobutyrate (SIB). 6.55 M, was prepared by adding NaOH (in D₂O) directly to neat isobutric acid (IBA). A series of solutions were obtained by mixing constant volumes of the SIB solution with increasing weights of neat IBA. This allowed for direct measurement of the weights of each component (using an analytical balance), which was more accurate for this careful work than is possible using volumes and densities (most micropipettes are calibrated for water, not for liquids with variable viscosities, and with densities far from 1.0 g/cm³). In each solution, the concentration of the SIB was kept constant, while the concentration of IBA increased incrementally. The series of solutions was prepared in such a way that constant volumes (8.3 μL of each) contained the same amount of SIB, but varying amounts of IBA. These small volumes were needed to minimize changes in field homogeneity, because shimming was carried out on the pure solutions of Na₃₄2 before start of each experiment, but not after additions of the isobutyrate buffer. For each kinetic measurement, Na₃₄2 (50 mg, 1.8 μM) and 490 μL of D₂O were placed in a 5 mm NMR tube. At t = 0 sec, 8.3 μL of the buffer solution was added, quickly shaken (t = 0 sec), placed in the NMR probe, and spinning was commenced immediately (final concentration of Na₃₄2 was 3.55 mM). At t = 60 sec, 1 pulse was acquired. Approach to equilibrium was followed to ensure that the kinetic run behaved as expected.



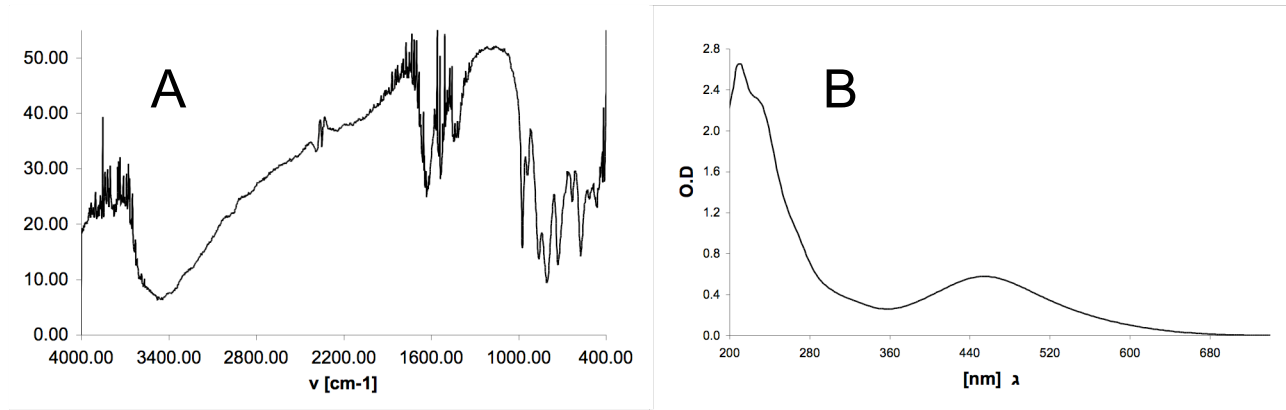
II. Figure S1. pH-Titration data showing the absence of ammonium acetate in Na₃₄2. Methane sulfonic acid (MSA) was added to solutions of (NH₄)₄₂1~10NH₄OAc (blue diamonds) and to solutions of Na₃₄2 (red squares). Buffering by NH₄OAc, evident in the upper plot (blue diamonds), is not observed when the acid is added to Na₃₄2 (red diamonds).



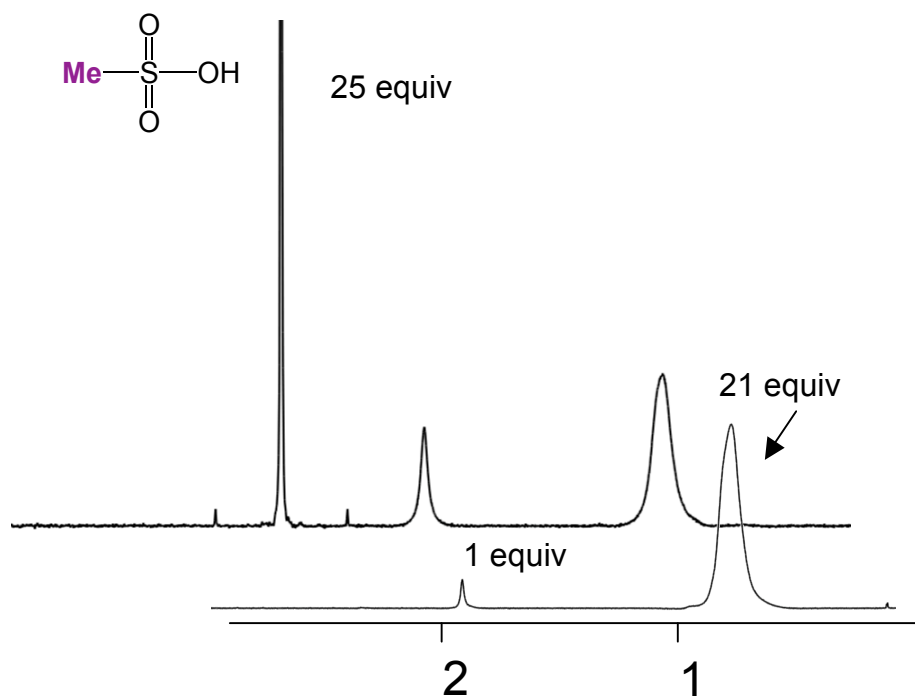
III. Figure S2. Comparison of the ^{13}C NMR spectra of $(\text{NH}_4)_{42}[\{\text{Mo}^{\text{VI}}_6\text{O}_{21}(\text{H}_2\text{O})_6\}_{12}\{\text{Mo}^{\text{V}}_2\text{O}_4(\text{OAc})\}_{30}]\cdot\sim 300\text{H}_2\text{O}\cdot\sim 10\text{CH}_3\text{COONH}_4$, and $\text{Na}_{34}\{(\text{Mo})\text{Mo}_5\}_{12}\{\text{Mo}_2\}_{30}(\text{CH}_3\text{CO}_2)_{22}(\text{H}_2\text{O})_{16}\}\cdot\sim 300\text{H}_2\text{O}$.



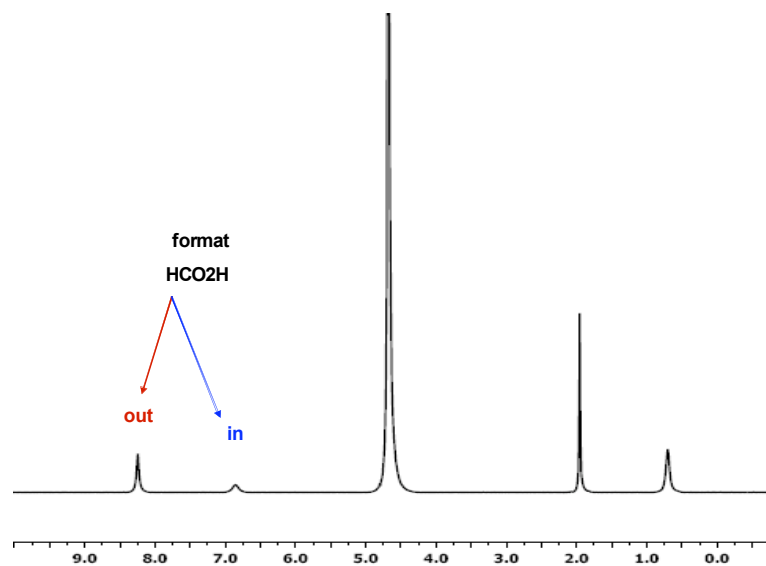
IV. Figure S3. The Raman spectrum of $\text{Na}_{34}\{(\text{Mo})\text{Mo}_5\}_{12}\{\text{Mo}_2\}_{30}(\text{CH}_3\text{CO}_2)_{22}(\text{H}_2\text{O})_{16}\}\cdot\text{ca. } 300\text{H}_2\text{O}$. The Raman bands observed for the metal-oxide framework of the Na^+ salt of **2** are effectively identical to those reported for the crystalline NH_4^+ salt (Müller, A.; Das, S. K.; Krickemeyer, E.; Kuhlmann, C.; Sadakane, M.; Dickman, M. H.; Pope, M. T. *Inorg. Synth.* **2004**, *34*, 191-200).



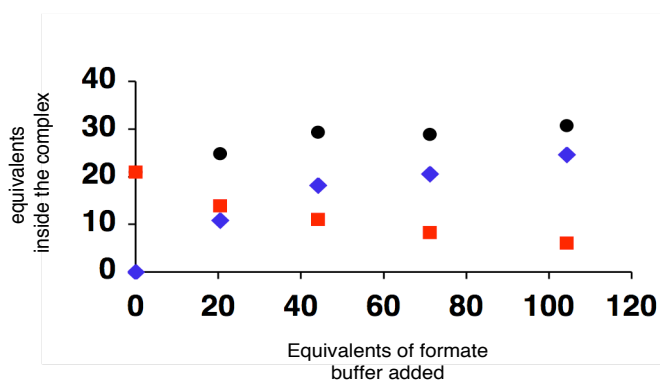
V. Figure S4. FTIR (top panel) and UV-vis (bottom panel) spectra of $\text{Na}_{34}\{(\text{Mo})\text{Mo}_5\}_{12}\{\text{Mo}_2\}_{30}(\text{CH}_3\text{CO}_2)_{22}(\text{H}_2\text{O})_{16}\} \cdot \text{ca. } 300\text{H}_2\text{O}$.



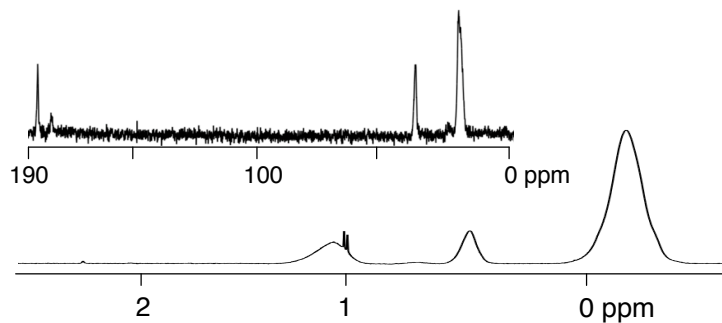
VI. Figure S5. This representative ¹H NMR spectrum shows how the number of equivalents of acetate in the Na⁺ salt of **2** was determined by quantitative addition of methanesulfonic acid (MSA). Here, ca. 25 equivalents of MSA have been added to a solution of the Na⁺ salt of **2**. Note: 1) The addition of the acid shifts the position of equilibrium of the reversible ligand-dissociation towards “free” acid (outside the complex), and 2) no signal from the MSA is observed inside the complex. This is true even when >80 equivalents of MSA are added (i.e., the signals are not coincident). If it were inside the complex, it should appear at ca. 1 ppm upfield, or at ca. 1.5 ppm.



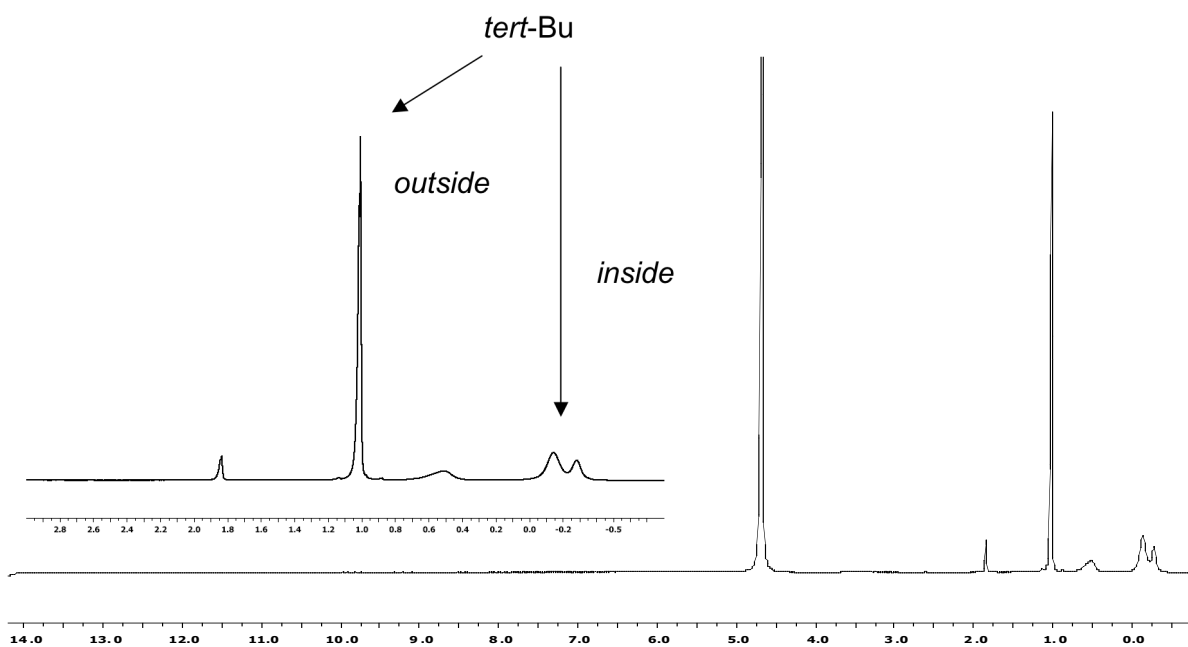
VII. Figure S6. This representative ^1H NMR spectrum shows equilibrated exchange between acetate and formate ligands.



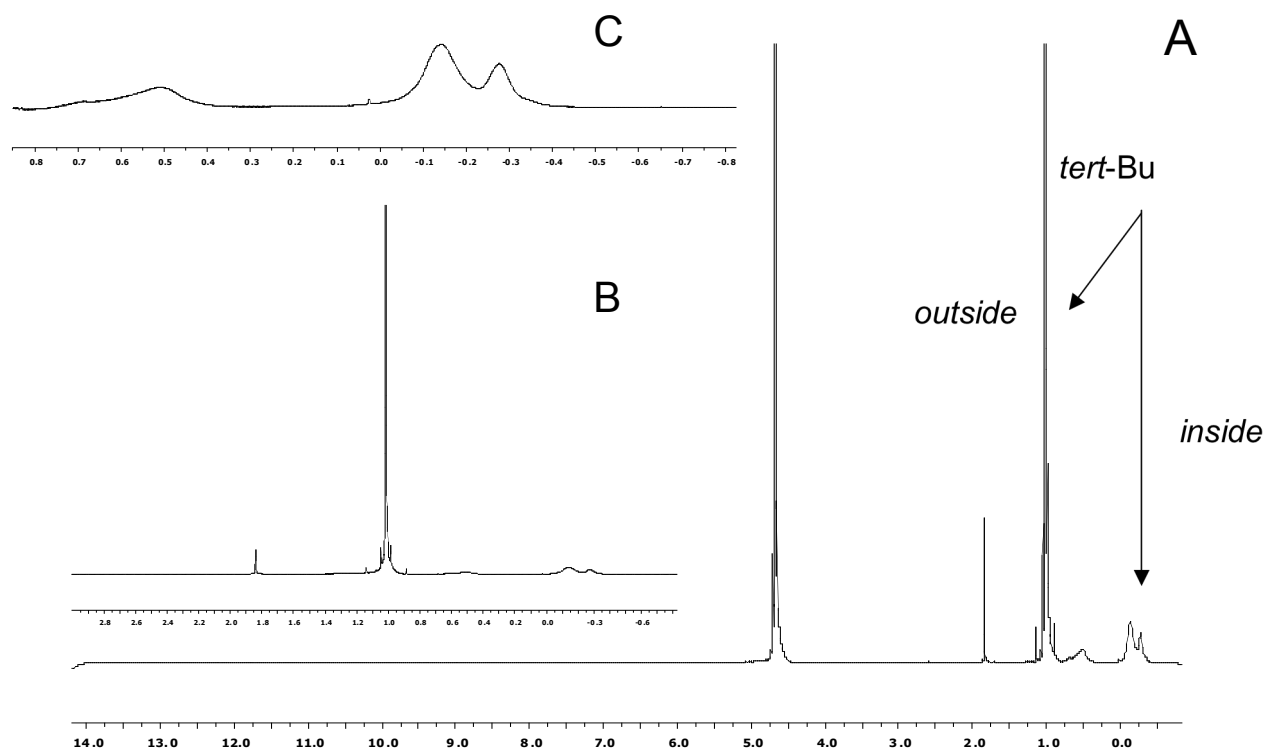
VIII. Figure S7. Equilibrium concentrations of acetate (red squares) and formate (blue diamonds) inside the complex after incremental additions of formate buffer to $\text{Na}_{24}\mathbf{2}$. The number of equivalents of acetate initially inside the complex (3.55 mM in D_2O) is 21. As the number of equivalents of 1:1 $\text{H}^+:\text{Na}^+$ formate buffer increases, acetate ligands are replaced by formate, and the total number of ligands inside (sum of acetate + formate) reaches its maximum value of ~ 30 (filled black circles). Note that when the concentration of acetate and formate (both forms of each) are nearly equal to one another, i.e., after addition of 20 equivalents of formate buffer, the concentrations of each inside the capsule are nearly identical. At this point, there are ~ 40 equivalents of potential ligands in the system, and due to dissociation equilibria, the total number of ligands is smaller than the maximum possible value of 30.



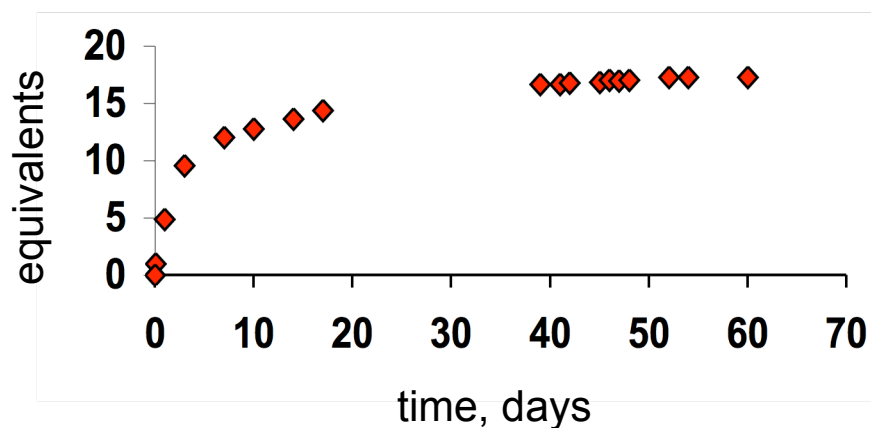
IX. Figure S8. Proton and ^{13}C NMR spectra (in D_2O) of the product obtained by replacement of most of the acetate in $\text{Na}_{34}\mathbf{2}$ by isobutyrate. The product was obtained by addition of 45 equiv. of 1:5 (*iso*- PrCO_2H :*iso*- PrCO_2Na) buffer to a D_2O solution of $\text{Na}_{34}\mathbf{2}$. After ~ 14 hours the solution was transferred to cellulose dialysis membrane, which was immersed in pure water for 90 min., after which the contents of the membrane were concentrated to dryness by rotary evaporation.



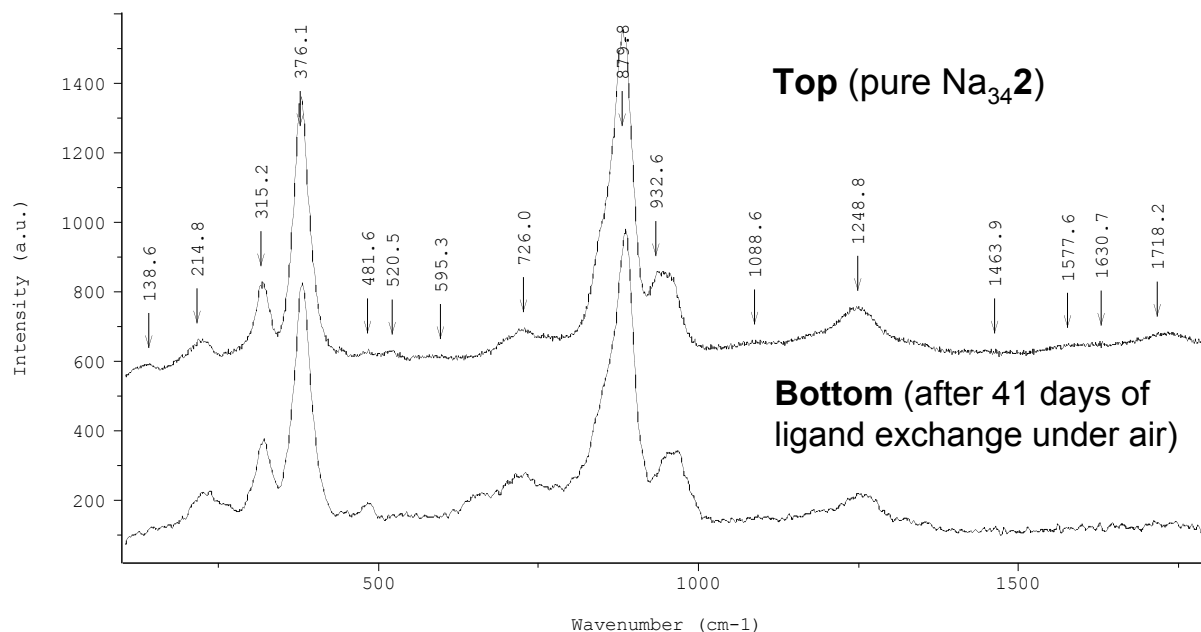
X. Figure S9. Proton-NMR spectrum of a D_2O solution containing $\text{Na}_{34}\mathbf{2}$ and 45 equiv. of trimethylacetic acid (1:1 buffer) after 41 days open to the air (prepared in aerated D_2O , and stored in the air in a gently capped NMR tube). **Inset:** expanded view of the upfield region. *This spectrum is effectively identical to that obtained when the reaction was carried out under strictly anaerobic conditions (Figure S10).* No signals other than that for HDO were observed farther downfield.



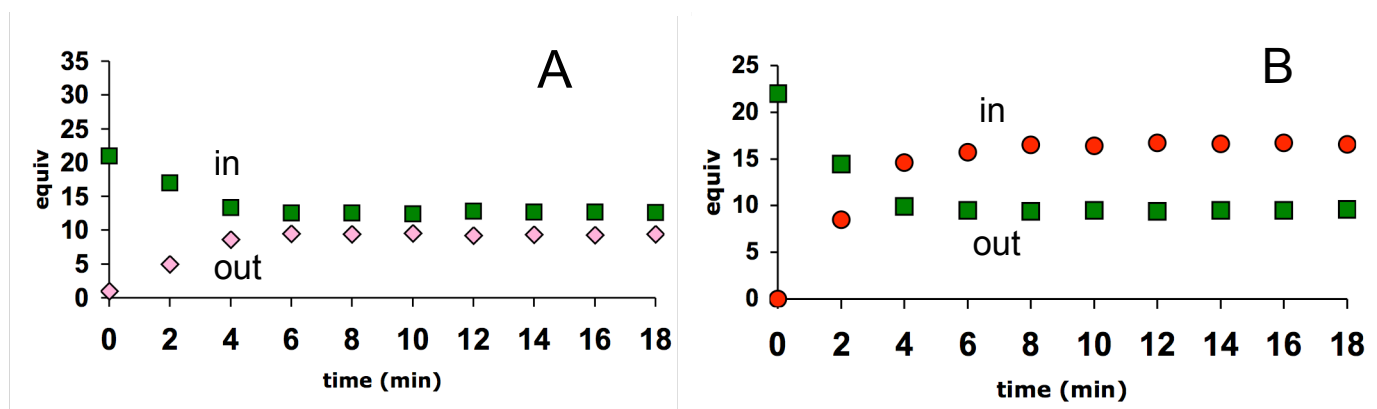
XI. Figure S10. Proton-NMR spectrum of a D_2O solution containing $Na_{34}2$ and 45 equiv. of trimethylacetic acid (1:1 buffer) after 25 days under strictly anaerobic conditions (N_2). **A:** full spectrum (some spinning side bands are present on the signal at 1 ppm), **B:** expanded view from -0.5 ppm to 3 ppm, **C:** expanded view of upfield region showing signals from acetate and isobutyrate ligands inside the complex (compare with Figure 5 in text).



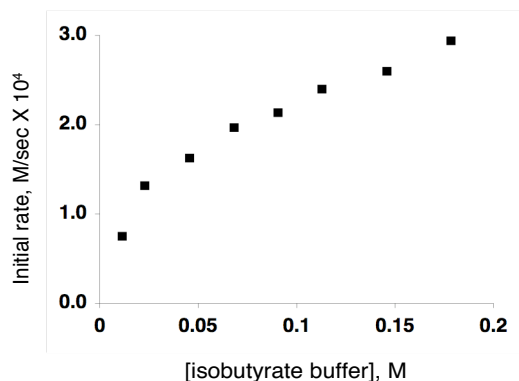
XII. Figure S11. Progress of reaction monitored by 1H NMR (D_2O) for equilibration via ligand exchange of $Na_{34}2$ and 33 equiv. of 1,1,1-trimethylacetic acid (1:1 buffer) in air. The plot shows the number of equivalents of 1,1,1-trimethylacetate ligand observed *inside* the capsule as a function of time. Spectra from this experiment are provided in Figure 5 in the text. (The NMR spectrometer was out of service for ~18 days in the middle of this experiment.)



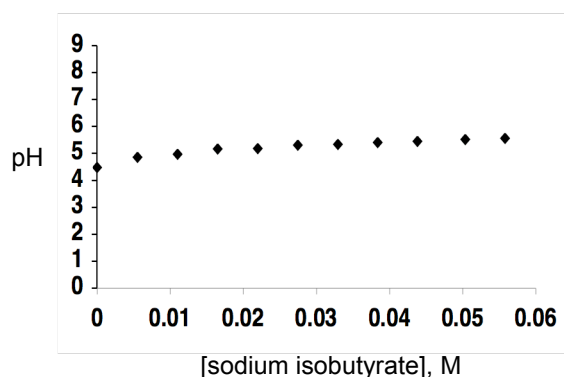
XIII. Figure S12. Raman demonstration of the stability of the oxomolybdate complex while undergoing dynamic ligand exchange in solution under aerobic conditions (air). **Top:** spectrum of solid Na₃₄2 (pure sample). **Bottom:** spectrum of the solid obtained after 41 days of reaction of 50 mg of Na₃₄2 in 0.5 mL D₂O with an excess of trimethylacetate buffer (1:1 H⁺:Na⁺), followed by concentration of the solution to a dry solid. *The molybdenum oxide structure is unchanged after 41 days of ligand-exchange equilibration under air.*



XIV. Figure S13. Equivalents of: **A:** acetate (Me signals by ¹H NMR) and of **B:** isobutyrate (*iso*-Pr signals by ¹H NMR), inside and outside the capsule after addition of 32 equivalents of 1:5 D⁺:Na⁺ isobutyrate buffer to an NMR tube containing a final concentration of 3.55 mM Na₃₄2 in D₂O. Two points deserved mention: 1) the approach to equilibrium involves sequential *different* reactions (each ligand exchange gives a new complex), and 2) at equilibrium ~29 of the 30 possible coordination sites are occupied by 12.5 acetate ligands and 16.5 isobutyrate ligands.



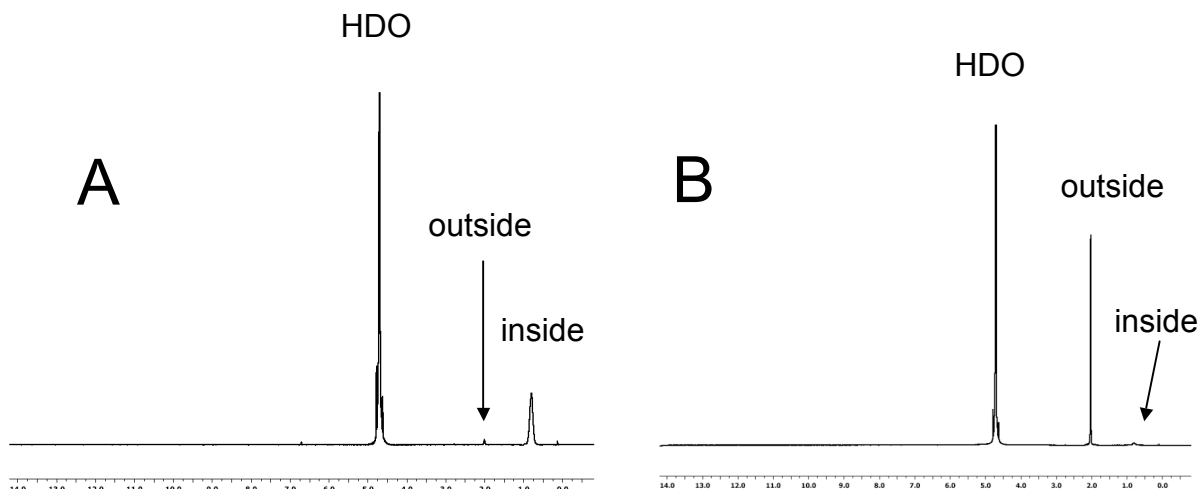
XV. Figure S14. Dependence of initial rates of ligand exchange on the concentration of added 1:5 RCO₂D:RCO₂Na (R = *iso*-Pr) in D₂O. Initial rates are [*iso*-PrCO₂⁻] observed *inside* the complex after the first 60 sec of the reaction.



XVI. Figure S15. Plot of pH values of an aqueous solution of Na₃₄2 (50 mg in 0.5 mL water) as a function of added isobutyrate (sodium salt). The concentrations shown on the x-axis are the amounts of isobutyrate actually added; the weak acid is clearly protonated to isobutyric acid in solution by Na₃₄2. When this was done in D₂O, the ¹H NMR of the solution showed no indication whatsoever of any degradation of 2.

Comments to Figure S15. The concentrations of isobutyrate added here exceed those added during kinetic studies reported here and in the text. In addition, if the same final (added) concentration of isobutyrate (ca. 0.05 M) is added to pure water, the pH climbs to 8.7. This concentration (0.05 M isobutyrate is similar to that used in the Figure 6 in the text (dependence on [RCO₂H] and constant [RCO₂Na]).

These data clearly show that isobutyrate is protonated by Na₃₄2, and therefore provide strong support for the argument made in the text that the non-zero (positive) y-intercept in the plot of initial rate vs. [RCO₂D] at constant added [RCO₂Na], is due to Brønsted acid-base conversion of RCO₂⁻ to RCO₂D by 2 acting as a “poly” aqua acid. ***When this same experiment was done in D₂O, the ¹H NMR of the solution showed no evidence whatsoever for degradation of 2.*** (Degradation, when it does occur, leads to clearly recognizable changes in the ¹H NMR spectra of the coordinated and free organic acids. None of these were observed.)



XVII. Figure S16. Effects of adding Na_2SO_4 and NaHSO_4 to D_2O solutions of $\text{Na}_{34}\mathbf{2}$ (100 mg/mL). **(A)** Addition of 60 equivalents of Na_2SO_4 . The pH (meter reading) was 4.3, and there was no evidence of ligand exchange. **(B)** Addition of 60 equivalents of NaHSO_4 leads to near-complete displacement of acetate (exchange) and a final pH (meter reading) of 1.4.

Comment to Figure S16. When Na_2SO_4 is added, the pH is effectively the same as that in solutions obtained by addition of isobutyrate buffers. Unlike for the carboxylate buffers, however, no exchange is observed. This shows that the protonation state of the entering ligand is kinetically significant, while the prevalent pH is not. When NaHSO_4 is added, by contrast, nearly complete exchange is observed even though there is virtually no neutral acid (H_2SO_4) present in solution (this is well known synthetic chemistry: Müller, A.; Rehder, D.; Haupt, E. T. K.; Merca, A.; *B. Angew. Chem. Int. Ed.* 2004, 43, 4466–4470). This highlights the role of protons in catalyzing the ligand exchange process, and provides an independent line of evidence that the non-zero y-intercept in Figure 6B is due to conversion of iso-PrCO_2^- to $\text{iso-PrCO}_2\text{D}$ by $\text{Na}_{34}\mathbf{2}$ acting as an aqua acid, rather than to the presence of two competing pathways, one for iso-PrCO_2^- (or $\text{iso-PrCO}_2\text{Na}$) and another for $\text{iso-PrCO}_2\text{D}$. Additional evidence is provided by the observation that when methanesulfonic acid (MeSO_3H) is added, no MeSO_3^- ligands are observed inside the capsule. While this ligand is weaker than SO_4^{2-} , we also suspect that it can't enter because of its low pK_a value (<-2). Because of this, it is "leveled" by D_2O to give effectively 100% conjugate base (MeSO_3^-), such that the concentration of the kinetically competent acid form is effectively zero.

XVIII. Concentrations of $\text{iso-PrCO}_2\text{D}$ in solution before and after the first 60 seconds of the reaction plotted in Figure 6B.

In the reaction plotted in Figure 6B, initial rates were determined after 60 seconds as a function of $\text{iso-PrCO}_2\text{D}$ at constant $[\text{iso-PrCO}_2\text{Na}]$ and constant $[\text{Na}_{34}\mathbf{2}]$. The following assumptions were used: 1) the ~1 acetate ligand in solution after dissolving $\text{Na}_{34}\mathbf{2}$ in D_2O at pH 4.5 was present as a 1:1 mixture of AcONa and AcOD , 2) $\text{Na}_{34}\mathbf{2}$, acting as an aqua acid converted 16.7% of the $\text{iso-PrCO}_2\text{Na}$ initially present (constant added concentrations of 0.049 M) to $\text{iso-PrCO}_2\text{D}$. This represents 2.3D^+ per equivalent of $\text{Na}_{34}\mathbf{2}$, 3) all the acid forms of the carboxylic acids present in the solution were equilibrating with one another via rapid acid-base equilibria in the bulk solution outside the oxomolybdate complex, and 4) the pK_a values of acetic acid and isobutyric acid are sufficiently close to one another (~0.1 pK_a unit) that the D^+ present was statistically distributed between these two species according to molar ratios in solution.

Then, ¹H NMR was used to determine the concentrations of methyl groups and isopropyl groups (from acid and conjugate-base anion forms of each) inside the capsule (anion forms) and outside (both acid and anion forms). Next, the concentration of $\text{iso-PrCO}_2\text{D}$ after 60 seconds was calculated as the fraction of $(\text{isobutyl}_{\text{out}}/\text{methyl}_{\text{out}}) \times$ total concentration of acid (sum of initially added $\text{iso-PrCO}_2\text{D}$ + 0.5 equiv from the labile acetate ligand + 2.3 from the oxomolybdate). In this calculation, the ratio $\text{isobutyl}_{\text{out}}/\text{methyl}_{\text{out}}$ corresponds to the total concentrations of each carboxylic acid and its conjugate base present in the bulk solution (these forms can't be differentiated from one another by ¹H NMR). The results are summarized in the following tables:

XIX. Table S1. Concentrations at $t = 0$ (after mixing all components)

Kinetic run	[<i>iso</i> -PrCO ₂ D] added, M	[<i>iso</i> -PrCO ₂ Na] added, M	actual [<i>iso</i> -PrCO ₂ D] at $t = 0$, M	actual [<i>iso</i> -PrCO ₂ Na] at $t = 0$, M
1	0.0061	0.0490	0.0161	0.0419
2	0.0101	0.0490	0.0201	0.0419
3	0.0152	0.0490	0.0252	0.0419
4	0.0202	0.0490	0.0302	0.0419
5	0.0243	0.0491	0.0343	0.0420
6	0.0323	0.0490	0.0423	0.0419
7	0.0352	0.0490	0.0451	0.0419

XX. Table S2. Concentrations after 60 seconds of reaction

Kinetic run	equiv acetate inside	equiv "Me" outside	equiv <i>iso</i> -PrCO ₂ ⁻ inside	equiv <i>iso</i> -Pr outside
1	19.74	2.26	2.92	12.60
2	18.78	3.22	4.04	12.62
3	18.60	3.40	5.05	13.03
4	18.25	3.75	5.73	13.76
5	18.23	3.77	6.42	14.26
6	17.32	4.68	8.75	14.17
7	16.58	5.42	9.04	15.19

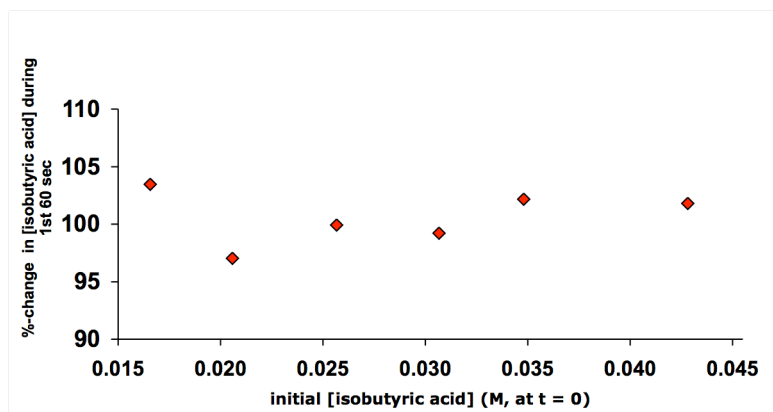
	[acetate] inside, M	["Me"] outside, M	[<i>iso</i> -PrCO ₂ ⁻] inside, M	[<i>iso</i> -Pr] outside, M
1	0.070	0.008	0.010	0.045
2	0.067	0.011	0.014	0.045
3	0.066	0.012	0.018	0.046
4	0.065	0.013	0.020	0.049
5	0.065	0.013	0.023	0.051
6	0.061	0.017	0.031	0.050
7	0.059	0.019	0.032	0.054

	["Me"] + [<i>iso</i> -Pr] outside, M	[AcOD] out, M	[<i>iso</i> -PrCO ₂ ⁻] out, M
1	0.053	0.002	0.014
2	0.056	0.004	0.016
3	0.058	0.005	0.020
4	0.062	0.006	0.024
5	0.064	0.007	0.027
6	0.067	0.011	0.032
7	0.073	0.012	0.033

From this data, it is possible to calculate the difference in concentrations of *iso*-PrCO₂D present in the bulk solution before and after the first 60 seconds of reaction. The formula used for this was:

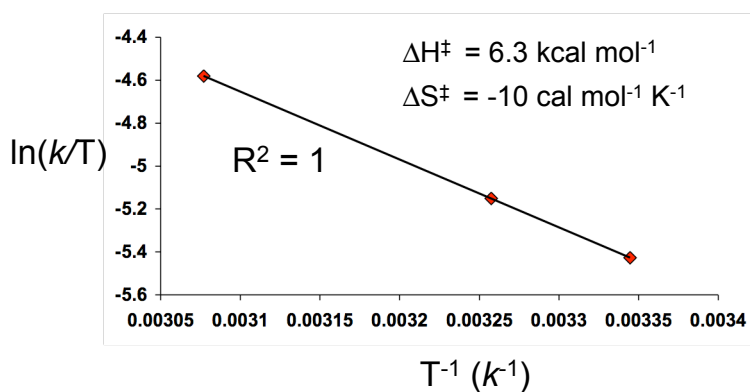
$$\text{Relative change (\%)} = \frac{([\textit{iso}\text{-PrCO}_2\text{D}]_{\text{after}} - [\textit{iso}\text{-PrCO}_2\text{D}]_{\text{before}})}{[\textit{iso}\text{-PrCO}_2\text{D}]_{\text{before}}} \times 100$$

The result is shown in Figure S17.



XXI. Figure S17. Percent change in isobutyric acid concentration in the bulk solution outside the complex before and after the first 60 seconds of reaction. In this plot, the initial concentration of *iso*-PrCO₂D is “100%”. Hence, the changes in concentration during the first 60 seconds are all within $\pm 5\%$ of the initial value.

As can be seen in the Figure, the concentration of isobutyric acid changed by $<5\%$ during each kinetic run. This is consistent with the acid form of the ligand acting as a catalyst. Because of this, each kinetic run was pseudo-zeroth order in the concentration of isobutyric acid, such that initial rates for each run were functions of the concentrations of isobutyric acid present at $t = 0$ seconds.



XXII. Figure S18. Eyring plot of preliminary temperature-dependence data obtained at constant $[Na_{3,4}2]$ ($= 1.8E-6$ M) and $[RCO_2D]$ (1:5 $H^+ : Na^+$ buffer, with $[buffer]_{tot} = 0.10594$ M), from 3 rate constants calculated from initial rates measured at 26, 34 and 56 °C.

This Eyring plot of preliminary temperature-dependence data (3 rate constants, obtained at 26, 34 and 56 °C; $R^2 = 1.00$) gave $\Delta H^\ddagger = 6.3$ kcal mol⁻¹ and $\Delta S^\ddagger = -10$ cal mol⁻¹ K⁻¹. These values are based on observed rate constants obtained from initial rates, rather than on rate-constants associated a well defined rate-limiting step. Hence, they include the temperature dependences of several acid-base equilibria, and must be interpreted with caution. However, the decrease in entropy fails to provide evidence that the rate-limiting step involves cleavage of Mo-O bonds.